FRACTOGRAPHIC IDENTIFICATION OF SUBCRITICAL TO CRITICAL CRACK GROWTH TRANSITION MECHANISMS IN CERAMICS

H. P. Kirchner and R. M. Gruver

Ceramic Finishing Company
Post Office Box 498
State College, Pennsylvania 16801

ABSTRACT

Variations in the relative proportions of intergranular and transgranular fracture and the distribution of other features such as projecting grains, pullouts, hummocks and depressions were investigated along radii from fracture origins in several polycrystalline ceramics. These variations were correlated with variations in the stress intensity factor (K_I) acting at the crack tip at various stages of subcritical crack growth. Objectives of the investigation included correlation of the frequencies of various microfracture processes with single crystal properties such as fracture energies for various cleavage plans, characterization of the mode of fracture at subcritical crack growth boundaries to determine criteria for locating these boundaries and identification of the micromechanisms controlling the transition from subcritical to critical crack growth.

In hot pressed alumina, minima in percent intergranular fracture vs. K_I curves occurred at K_I values that were approximately equal to the K_{IC} values for fracture on particular lattice planes. The primary (lowest) minimum occurred at $K_I \cong K_{IC}$ for the polycrystalline material, providing a criterion for locating the subcritical crack growth boundary. In coarser grained aluminas, these boundaries were marked by projecting grains and holes caused by pullouts. In hot pressed silicon nitride, the fracture origins were surrounded by flat regions of transgranular fracture which, in turn, were surrounded by regions of hummocks and depressions which marked the subcritical crack growth boundary. Transformation toughened zirconia, available as a very coarse grained body, fractured transgranularly with few distinctive features.

KEYWORDS

Fractography; ceramics; microfracture mechanisms; intergranular and transgranular fracture; subcritical crack growth; criteria for critical flaw boundaries.

INTRODUCTION

In ceramics, cracks propagate at a wide range of stress intensity factor (K_I) values ranging from K_o, the threshold value for crack growth under stress corrosion conditions, to K_B, the stress intensity factor at crack branching. The strain

energy available for crack propagation increases with K_I. At low crack velocities ($K_I < K_{IC}$),[1] where the energy required for acoustic wave propagation from the crack tip and for kinetic energy of the material near the crack is small, these differences in available strain energy cause variations in the micromechanics of the fracture process.

The principal assumption on which this investigation was based is that the fracture energy for the advancing crack is the sum of the fracture energies of the individual microfractures occurring at the crack front (Kirchner and Gruver, 1979). There are substantial variations in the fracture energies of the various micromechanisms. Therefore, as the K_I increases one expects increasing frequencies of occurrence of the micromechanical mechanisms requiring higher fracture energies. These variations in the frequencies should be observable by conventional techniques of fractography.

In this investigation, fracture origins in several structural ceramics including alumina, silicon nitride and zirconia bodies, were identified and characterized by scanning electron microscopy (SEM). The fracture surfaces were characterized along radii from the fracture origins. The relative amounts of intergranular and transgranular fracture were determined at intervals along these radii by placing a grid over a composite photograph of the fracture surface and evaluating the fracture surface in each grid space. The results were averaged for each interval and expressed in terms of percent intergranular fracture (PIF). The variations in PIF were correlated with the K_I acting at the crack front at each stage of crack growth (interval). In addition, the crack radii to the critical flaw boundaries ($K_I = K_{IC}$) were calculated and the fracture surfaces were examined along the boundaries determined by these radii to identify features that might be used as criteria for locating these boundaries or that might be used to identify the microfracture mechanisms that are responsible for the transition from subcritical to critical crack growth.

RESULTS AND DISCUSSION

Three different grades of alumina were investigated including LUCALOX[2], a rather coarse grained (30 μm) semi-transparent material; ALSIMAG 614[3], a finer grained (5 μm) 96% alumina; and a hot pressed (HP) alumina, with a grain size of about 1-3 μm prepared at Ceramic Finishing Company. The results for these three grades of alumina are given in the following sections and are followed by results for silicon nitride and zirconia.

H.P. Alumina

When viewed by reflected light in an optical microscope, fracture origins in HP alumina, as well as many other ceramics, are surrounded by reflecting spots. Comparison of the sizes, shapes and locations of these reflecting spots with areas of transgranular fracture observed by SEM shows that the reflecting spots are caused by reflections from areas of transgranular fracture. The reflecting spots provide the most reliable means for locating the fracture origins.

[1] K_{IC} is the critical stress intensity factor.

[2] LUCALOX, General Electric Company, Cleveland, OH.

[3] ALSIMAG 614, 3 M Company, Chattanooga, TN.

The areas containing reflecting spots are larger for weaker specimens and those fractured by delayed fracture testing than they are for stronger specimens and those fractured by impact. Therefore, the variations in the areas are related to a K_I at the crack tip and the extent of subcritical crack growth (Kirchner and Richard, 1980).

The PIF was determined at intervals along radii from fracture origins in HP alumina (Kirchner and Gruver, 1979). The K_I acting at the crack tip during each interval of crack growth was calculated using

$$K_I = \frac{Y}{Z} \sigma_F a^{1/2} \qquad (1)$$

in which σ_F is the fracture stress, a is the crack depth, Y is a geometrical factor which is taken as 2 for surface cracks, and Z is the flaw shape parameter which can be taken from a graph in Evans and Tappin (1972). Specimens with well defined fracture origins and symmetrical areas of reflecting spots were selected for investigation to minimize the inaccuracies in the K_I estimates.

PIF vs. K_I curves were plotted. In delayed fracture specimens in which there is extensive subcritical crack growth, these curves show several maxima and minima in PIF (Fig. 1). The minima occur at K_I values that are approximately equal to the K_{IC} values for fractures on various crystal planes in sapphire crystals (Weiderhorn, 1969, 1974; Becher, 1976) as illustrated in Table 1. The K_{IC} values in Table 1 were estimated using fracture energies from the above references, assuming a constant value of Young's modulus.

The fact that the K_I values at the minima in PIF correspond to the K_{IC} values for fracture on the various crystallographic planes in sapphire is interpreted to mean that, as the K_I at the crack tip passes each threshold at which fracture on a particular lattice plane can occur, the fraction of transgranular fracture increases. When the crystals at the crack front that are suitably oriented for fracture on this plane have fractured, no additional fracture energy can be adsorbed by this mechanism so the crack velocity and PIF increase until K_I increases to the point that another transgranular fracture mechanism becomes available. Then, there is another trend toward transgranular fracture and the cycle repeats itself.

Other specimens were fractured at a higher loading rate and at 800°C. At the increased loading rate the details of the peaks and valleys were obscured because of the reduction in the amount of subcritical crack growth. However, the primary minimum was still evident. At 800°C, the K_I vs. PIF curve was shifted to higher PIF but, again, the primary minimum was evident.

At room temperature the K_{IC} of fine grained, HP alumina is approximately 4.2 $MPa \cdot m^{1/2}$. The above results suggest that the primary minimum in PIF at 4.3 $MPa \cdot m^{1/2}$ can be used to locate the subcritical crack growth boundary and that the transition from subcritical to critical crack growth occurs when additional fracture energy can no longer be absorbed by transgranular fracture on $\{\bar{1}126\}$ lattice planes at 4.3 $MPa \cdot m^{1/2}$.

96% Alumina

The 96% alumina has a larger average grain size than the HP alumina. The larger grain size increases the tendency toward transgranular fracture, perhaps because of the increased energy required for the relatively large deviations of the crack

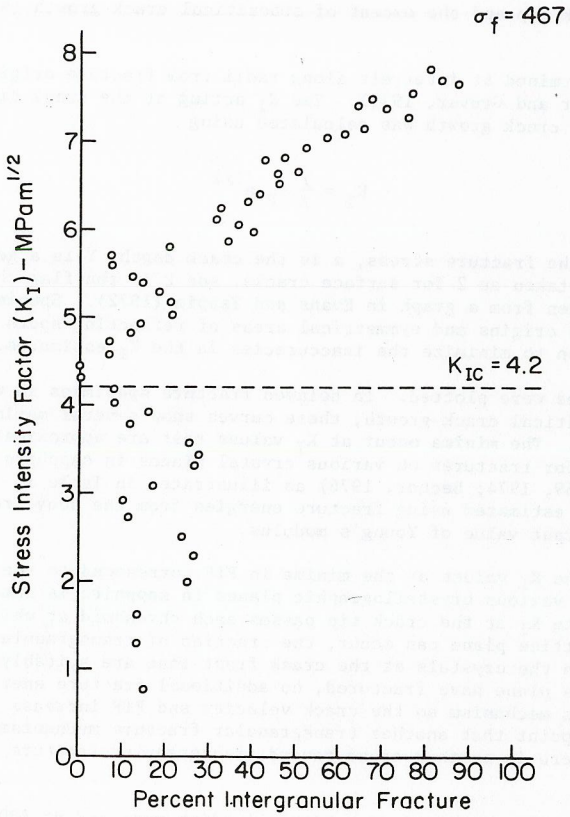

Fig. 1. Stress intensity factor vs. percent intergranular fracture, delayed fracture (hot pressed alumina specimen D-12). Republished with permission of Journal of Materials Science, Chapman and Hall, Ltd., Publishers.

from the average plane of propagation that would be required for intergranular fracture to occur. This increased transgranular fracture means that, at times, the percent transgranular fracture is so near to 100% that it is difficult for the minima in PIF to manifest themselves. As in the case of HP alumina, the fracture origins are surrounded by reflecting spots (Kirchner and Gruver, 1980). In some cases, the fracture origins in 96% alumina were also surrounded by a region of projecting grains and pullouts.

The PIF was determined at intervals along the radii from the fracture origins and the stress intensity factors, acting at each of these intervals during crack growth,

TABLE 1 Comparison of K_{IC} Values for Lattice Planes in Sapphire and K_I Values at Minima in PIF

Lattice Plane	K_{IC} for Lattice Plane MPa·m$^{1/2}$	K_I at Minimum in PIF MPa·m$^{1/2}$
$\bar{1}012$	2.15 (1.7)	1.7
$10\bar{1}0$	2.4	2.9
$\bar{1}126$	4.3	4.3
0001[4]	>5.6	5.6

were calculated. Graphs of K_I vs. PIF revealed that, in many cases, the primary minimum in PIF was observed when $K_I \simeq K_{IC}$ where K_{IC} is 3.8 MPa·m$^{1/2}$. However, in some cases the maxima and minima in PIF were not observed and there was a gradual increase in PIF beginning at $K_I \simeq 3$ MPa·m$^{1/2}$.

Based on the above evidence, there seem to be two types of failure mechanisms in this 96% alumina. In the first type the boundary at which $K_I = K_{IC}$ occurs at the minimum in PIF as in H.P. alumina and it may also be marked by a line of projecting grains and pullouts. In the second type, the boundary can be taken at the K_I value where the consistent increase in PIF begins. In this case, the localized K_{IC} may be lower than the K_{IC} determined for large cracks. A possible explanation of this effect is that there are areas of grains with preferred orientations favoring crack growth, so that the localized (small crack) K_{IC} is smaller than the K_{IC} values determined by conventional techniques using large cracks. The fractures will tend to seek out these areas because the lower resistance to fracture will permit more extensive subcritical crack growth so that these regions are more likely to become critical flaws.

LUCALOX alumina

LUCALOX has an average grain size of 30 μm and is the coarsest grained alumina investigated. A fracture surface of LUCALOX fractured at 345 MPa is illustrated in Fig. 2. Both halves of the specimen are shown with the fracture origin in the center of the top edge of the specimen, perhaps at the indentation that seems to contain a small number of fragments.

The fracture origin is surrounded by an area of mixed transgranular and intergranular fracture. In the top photograph, this area is bounded by a row of projecting grains located in a semi-elliptical line with a minor axis of about 80 μm extending from the flaw to the boundary. In the matching photograph below where the negative was reversed so that the horizontal positions are the same in both photographs, the positions of the holes caused by the pullouts match those of the projecting grains above.

The stress intensity factor (K_I) at the boundary formed by the projecting grains was calculated. Depending on the exact value of the crack depth selected and the

[4]Weiderhorn (1969) indicates that instead of fracturing on the {0001} lattice plane, fractures in sapphire tend to alternate between two fracture modes; transgranular fracture on {$\bar{1}012$} planes and conchoidal fracture roughly parallel to the {$0\bar{1}14$} plane.

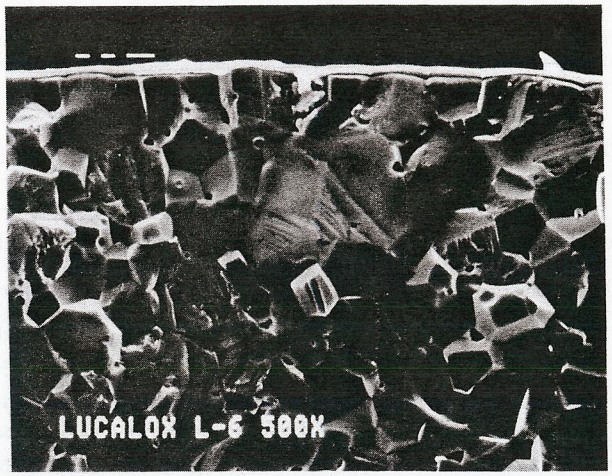

(A) Fracture surface showing projecting grains.

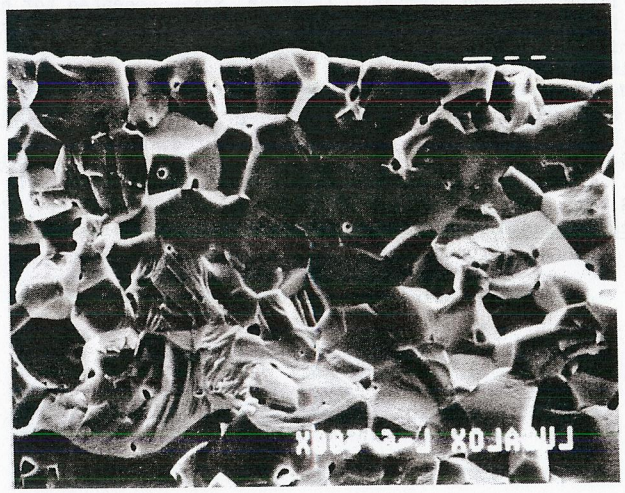

(B) Mating fracture surface showing holes caused by pullouts.

Fig. 2. Fracture surfaces in LUCALOX (the longest white lines at the tops of the photographs are 10 μm long).

value of Z taken for the ellipse, the K_I values ranged downward from 4.5 MPa·$m^{1/2}$. Measured K_{IC} values for LUCALOX range from 4.1 to 4.9 MPa·$m^{1/2}$ (Freiman, McKinney, and Smith, 1974; Evans, Linzer, and Russell, 1974). Therefore, the present evidence indicates that the projecting grains and pullouts mark the subcritical crack growth boundary in this specimen and that the mechanism controlling transition from subcritical to critical crack growth involves pulling grains out of the fracture surface. These particular grains are probably those that are oriented so that the planes with orientations parallel to the fracture surface are resistant to transgranular fracture.

H.P. Silicon Nitride

Silicon nitride specimens[5] with carefully polished surfaces were fractured in uniaxial tension at room temperature (Kirchner, Gruver, and Richard, 1979). All of the fractures originated at internal flaws that appeared to be inclusions or inclusions associated with small pores. Each fracture origin is surrounded by a relatively flat region of primarily transgranular fracture. These flat regions are elliptical in shape and vary in ellipticity from specimen to specimen. In some orientations in the SEM, the flat regions are dark and have a distinctive and well-defined appearance.

As a first approximation, it was assumed that the subcritical crack growth boundary coincided with the outer boundary of the flat region and the K_I values at the intersections of the major and minor axes with this outer boundary were calculated. The larger values (at the minor axis intersections) were too low, on the average, to be consistent with the subcritical crack growth boundary.

Further examination of the fracture surfaces revealed that the flat regions are surrounded by regions of hummocks and depressions. These features are elongated along radii from the fracture origin but are not hackle which occur much farther from the fracture origin. As a second approximation, the subcritical crack growth boundary was assumed to coincide with the outer edge of the first row of hummocks and depressions. The stress intensity factors at the intersections of the major and minor axes with the boundary were calculated. In this case, the average of the highest K_I values (at the minor axis intersections) was 4.8 MPa·$m^{1/2}$ which is approximately equal to the K_{IC} of the body which is 4.7 MPa·$m^{1/2}$ (Petrovic, Jacobson, Talty, and Vasudevan, 1975).

These results indicate that the outer edge of the first row of the hummocks and depressions is the subcritical crack growth boundary. Apparently, the hummocks consist of agglomerates of elongated grains that are oriented more or less perpendicular to the crack. These agglomerates are resistant to the crack growth so that the cracks tend to pass over or under the agglomerates forming the hummocks and depressions.

Transformation Toughened Zirconia (TT-ZrO_2)

Calcia partially stabilized zirconia specimens[6], aged in the cubic-tetragonal phase field at 1300°C for various times, were fractured in flexure (Kirchner, Gruver, Swain, and Garvie, 1980). As is well known, crack propagation in TT-ZrO_2 leads to transformation from tetragonal to monoclinic ZrO_2 at the crack tip which, in turn, results in high values of K_{IC}; hence, the term transformation toughened. These particular specimens consisted of very large grains (50 μm) of cubic zirconia containing a fine precipitate of tetragonal ZrO_2.

[5]NC-132 Norton Company, Worcester, MA, average grain size 1-2 μm.

[6]TT-ZrO_2 specimens furnished by Mr. R. C. Garvie, CSIRO, Melbourne, Australia.

Fracture surfaces of these specimens were characterized. Reflecting spots were used to locate the fracture origins. In some cases the flaws at the fracture origins were identified and characterized. The fracture surfaces consisted almost entirely of transgranular fracture. The fracture surface was smooth near the fracture origin and became increasingly wavy and rough with increasing distance from the fracture origin.

The strong tendency toward transgranular fracture in TT-ZrO_2 is believed to be caused by the large grain size. The energy required to propagate a crack around such a grain is very large because the crack must depart so much from its otherwise normal path of propagation. Criteria for locating subcritical crack growth boundaries have not yet been determined for the material, primarily because the fracture surfaces lack distinctive features.

SUMMARY AND CONCLUSIONS

Strong evidence showing that the frequencies of fracture of grains by various micromechanisms depend on the K_{IC} values of the individual microfractures (fracture on various lattice planes) and the K_I acting at the crack front, was obtained for fine grained polycrystalline alumina specimens. The dependence on K_I results in substantial variations in the mode of fracture along radii from fracture origins. The fracture origins are surrounded by reflecting spots which correspond to regions of transgranular fracture. Apparently, when K_I and crack velocity are low, transgranular fracture is favored. However, as the crack speeds up there is increasing intergranular fracture with the crack going around the smaller grains and through the larger grains, at least those with favorable orientations, thus minimizing the energy necessary for intergranular fracture. At high values of K_I (crack velocity) there is a strong trend toward intergranular fracture.

Criteria were determined for locating subcritical crack growth boundaries in several ceramics. These criteria are described in Table 2.

TABLE 2 Fractographic Criteria for Locating Subcritical Crack Growth Boundaries in Various Ceramics

Ceramic Body	Grain Size μm	Criteria for Locating Subcritical Crack Growth Boundaries
HP Alumina	1-3	Primary minimum in PIF
96% Alumina (ALSIMAG 614)	5-7	Primary minimum in PIF Projecting grains and pullouts
LUCALOX Alumina	30	Projecting grains and pullouts
HP Silicon Nitride (NC-132)	1-2	Boundary formed by hummocks and depressions
Transformation Toughened Zirconia	50	None determined

In 96% alumina and probably in other ceramics, the increasing plastic deformation at the crack tip, as K_I increases above K_{IC}, is evident in the fracture features. After applying the criteria in Table 2, the location of the selected boundary can be compared with the locations of these plastic deformation features that occur at greater radii, to confirm the selected boundary.

ACKNOWLEDGEMENT

The writers are pleased to acknowledge the contributions of their associates at Ceramic Finishing Company, especially D. M. Richard, and at CSIRO, especially R. C. Garvie, and the sponsorship of the Naval Air Systems Command.

REFERENCES

Becker, P. F. (1976). Fracture strength anisotropy of sapphire. J. Amer. Ceram. Soc., 59, 59-61.

Evans, A. G. and G. Tappin. (1972). Effects of microstructure on the stress to propagate inherent flaws. Proc. Brit. Ceram. Soc., 20, 275-297.

Evans, A. G., M. Linzer, and L. R. Russell. (1974). Acoustic emission and crack propagation in polycrystalline alumina. Mater. Sci. and Eng., 15, 253-261.

Freiman, S. W., K. R. McKinney, and H. L. Smith. (1974). Slow crack growth in polycrystalline ceramics. Fracture Mechanics of Ceramics, Vol. 2, Plenum, New York, pp. 659-676.

Kirchner, H. P. and R. M. Gruver. (1979). A fractographic criterion for subcritical crack growth boundaries in hot-pressed alumina. J. Mater. Sci., 14, 2110-2118.

Kirchner, H. P. and R. M. Gruver. (1980). Fractographic criteria for subcritical crack growth boundaries in 96% alumina. J. Amer. Ceram. Soc., 63, 169-174.

Kirchner, H. P., R. M. Gruver, and D. M. Richard. (1979). A fractographic criterion for subcritical crack growth boundaries at internal fracture origins in hot-pressed silicon nitride. J. Mater. Sci., 14, 2713-2720.

Kirchner, H. P. and D. M. Richard. (1980). Fracture stress reflecting spot relations in hot pressed alumina. J. Mater. Sci. Accepted for publication.

Kirchner, H. P., R. M. Gruver, M. V. Swain, and R. C. Garvie. (1980). Crack propagation and branching in transformation toughened zirconia. Submitted for publication.

Petrovic, J. J., L. A. Jacobson, P. K. Talty, and A. K. Vasudevan. (1975). Controlled surface flaws in hot pressed Si_3N_4. J. Amer. Ceram. Soc., 58, 113-116.

Wiederhorn, S. M. (1969). Fracture of sapphire. J. Amer. Ceram. Soc., 52, 485-491.

Wiederhorn, S. M. (1979). Subcritical crack growth in ceramics. Fracture Mechanics of Ceramics, Vol. 2, Plenum, New York, pp. 613-646.